NeuroImage 202 (2019) 116095

Contents lists available at ScienceDirect

NeuroImage

journal homepage: www.elsevier.com/locate/neuroimage

Adjusting gait step-by-step: Brain activation during split-belt treadmill walking

Dorelle C. Hinton [a,b], Alexander Thiel [c,d], Jean-Paul Soucy [c], Laurent Bouyer [e,f], Caroline Paquette [a,b,*]

[a] Department of Kinesiology and Physical Education, McGill University, Montreal, H2W 1S4, Canada
[b] Centre for Interdisciplinary Research in Rehabilitation of Montreal (CRIR), Montreal, H3S 1M9, Canada
[c] Department of Neurology and Neurosurgery, McGill University, Montreal, H3A 2B4, Canada
[d] Lady Davis Institute for Medical Research, Jewish General Hospital, Montreal, H3T 1E2, Canada
[e] Centre for Interdisciplinary Research in Rehabilitation and Social Integration (CIRRIS), Quebec, G1M 2S8, Canada
[f] Department of Rehabilitation, Faculty of Medicine, Université Laval, Quebec, G1V 0A6, Canada

ARTICLE INFO

Keywords:
Split-belt treadmill
^{18}FDG PET imaging
Locomotor plan
Gait alterations

ABSTRACT

When walking on a split-belt treadmill, where each leg is driven at a different speed, a temporary change is made to the typical steady-state walking pattern. The exact ways in which the brain controls these temporary changes to walking are still unknown. Ten young adults (23±3y) walked on a split-belt treadmill for 30 min on 2 separate occasions: tied-belt control with both belts at comfortable walking speed, and continuous adjustment where speed ratio between belts changed every 15 seconds. ^{18}F-fluorodeoxyglucose (^{18}FDG) positron emission tomography (PET) imaging measured whole brain glucose metabolism distribution, or activation, during each treadmill walking condition. The continuous adjustment condition, compared to the tied-belt control, was associated with increased activity of supplementary motor areas (SMA), posterior parietal cortex (PPC), anterior cingulate cortex and anterior lateral cerebellum, and decreased activity of posterior cingulate and medial prefrontal cortex. In addition, peak activation of the PPC, SMA and PFC were correlated with cadence and temporal gait variability. We propose that a "fine-tuning" network for human locomotion exists which includes brain areas for sensorimotor integration, motor planning and goal directed attention. These findings suggest that distinct regions govern the inherent flexibility of the human locomotor plan to maintain a successful and adjustable walking pattern.

1. Introduction

The ability to quickly alter and fine tune one's walking pattern requires asymmetrical adjustments in the patterns of step length, stance and swing between legs. In the laboratory, a split-belt treadmill, with independently driven belts under each leg, can recreate the separate functions of each leg, similar to those occurring during rapid changes to the walking pattern. When belts suddenly start moving at different speeds without warning to the participant (split-belts), a spontaneous reactive change must be made to the previous typical symmetrical steady-state walking pattern. However, with extended exposure to split-belts, feedforward anticipatory gait control integrates ongoing sensorimotor information to update the motor plan, gradually allowing the central nervous system to create a context-specific locomotor program (Blanchette and Bouyer, 2009; Reisman et al., 2010). The ability to react to, and learn from, treadmill belts operating at different speeds highlights the nervous system's capacity to alter locomotion to perturbations from the environment. The exact neural correlates underlying these locomotor program adjustments are now only beginning to emerge.

Thus far, hypotheses of the neural control underlying reactive and anticipatory gait alterations to spilt-belt treadmill walking have been primarily based on studies of clinical populations. Within 5 steps of walking on split-belts, gait cycle changes are present in subjects with damage to the midline cerebellum (Morton and Bastian, 2006), cortical strokes (Reisman et al., 2005), children who underwent hemispherectomy (Choi et al., 2009), Parkinson's disease (PD) patients (Dietz et al., 1995) and even healthy infants prior to independent stepping (Yang et al., 2005). While these reactive gait changes are not affected, feedforward anticipatory gait cycle changes necessary for adaptation are not fully functioning in these populations, highlighting that cerebellar and supratentorial regions are required for learning a new locomotor pattern.

Anticipatory changes to the gait pattern occur as a result of a change

* Corresponding author. Department of Kinesiology and Physical Education, McGill University, Montreal, H2W 1S4, Canada.
E-mail address: caroline.paquette@mcgill.ca (C. Paquette).

https://doi.org/10.1016/j.neuroimage.2019.116095
Received 13 May 2019; Received in revised form 9 August 2019; Accepted 11 August 2019
Available online 17 August 2019

in the motor plan from repeated exposure to the reactive gait changes with the goal of minimizing errors. la Fougere and colleagues (la Fougere et al., 2010) hypothesized that this error driven feedback would originate from the spinal cord, through cerebellum to brainstem and basal ganglia, and would create a functional loop with the supplementary motor areas (SMA). This would allow for alterations to the ongoing motor plan through the brainstem and for updates to environmental constraints (la Fougere et al., 2010). This functional network for planned walking modifications has been confirmed with other neuroimaging studies involving locomotion, suggesting that sensorimotor integration while walking would not only require cortical activation of SMA (Miyai et al., 2001; Suzuki et al., 2008) but would also involve the posterior parietal cortex (PPC) (Lajoie et al., 2010; Gwin et al., 2011; Billingston et al., 2013; Drew and Marigold, 2015; Mitchell et al., 2018; Wong and Lomber, 2019) and primary motor and somatosensory areas (Fukuyama et al., 1997; Miyai et al., 2001; Suzuki et al., 2008; Gwin et al., 2011). Finally, lateral cerebellar areas have been implicated in goal directed, or anticipatory, foot placement changes (Ilg et al., 2008) and adaptation of the gait pattern to split-belt walking (Morton and Bastian, 2006) while midline cerebellar lesions indicate that this region has a role in the dynamic postural control required during typical straight walking (Bastian et al., 1998). In addition to further cortical activation, the healthy CNS also reduces activity in areas known to be part of the Default Mode Network (DMN) during task performance (Raichle et al., 2001). The DMN is active at rest and involved in self-reference, memory and thought and deactivates when any motor tasks are performed including walking (Crockett et al., 2017).

Previous studies suggest that anticipatory gait changes to split-belt treadmill walking, but not reactive gait changes, are affected by cerebellar, cerebral or subcortical damage. This raises the question of whether it is possible that part of the underlying neural control for reactive gait changes is located within lower level structures such as the brain stem, vestibulo-spinal portions of the cerebellum and spinal cord? A more direct assessment of the healthy central nervous system responses to split-belt walking, using functional neuroimaging for instance, could help provide a more detailed description of its control mechanism.

By means of the progressive accumulation of a radioactive glucose analog to map whole brain metabolism, neural activity imaged with ^{18}F-fluorodeoxyglucose (^{18}FDG) positron emission tomography (PET) represents the brain's average activity over a 30 to 40-min period. While this excludes ^{18}FDG PET for assessing events that take place over a short period of time, it does allow for the assessment of activities sustained over the entire uptake period, such as walking. Previous ^{18}FDG PET protocols have successfully generated hypothesizes of the brain areas involved when modulation of the gait pattern is required (la Fougere et al., 2010; Mitchell et al., 2018).

Using ^{18}FDG PET imaging, this project identified cerebral and cerebellar brain regions involved in the control of continuous gait modifications needed to successfully perform a split-belt treadmill task in healthy young adults. We hypothesized that continuous gait modifications to changing inter-belt speed ratios on the split-belt treadmill would increase levels of glucose metabolism (i.e. would recruit) areas involved in sensorimotor feedback integration and goal-directed foot placement: the lateral portions of the cerebellum, supplementary motor areas and the posterior parietal cortex.

2. Materials and methods

2.1. Subjects

Ten healthy, young adults (mean age = 22 ± 3 years, 5 male) with normal or corrected-to-normal vision and no history of diabetes, vestibular dysfunction, neurological, musculoskeletal or cardiopulmonary disorders participated in this study. All participants had experience walking on a regular treadmill but were naïve to walking on a split-belt treadmill before their participation in this study. The experimental protocol was approved by the McGill Institutional Review Board and all participants provided written consent.

2.2. Equipment

For gait analysis, participants wore seven wireless inertial measurement units (IMUs; triaxial accelerometers, gyroscopes and magentometers; Opal™, APDM Inc., Portland, OR) on the sternum, forehead, sacrum, left and right wrist, and left and right lower shank. A split-belt treadmill (Forcelink Dual Belted Treadmill on N-Mill Frame) consisting of two independently-operating belts separated by a 5 cm gap and three safety bars (front, right and left sides) was used to induce a continuous speed change to the gait pattern (Supplementary Fig. 1). While walking on the treadmill, participants wore a safety harness for fall protection that provided no mechanical support nor hindered movements. To compensate for differences in treadmill belt noise at different speeds, participants wore binaural over-ear headphones which played pure white noise while walking.

2.3. Laboratory familiarization visit

Participants first provided signed informed consent, completed questionnaires for Positron Emission Tomography (PET) and Magnetic Resonance Imaging (MRI) and completed the International Physical Activity Questionnaire (IPAQ, Craig et al., 2003). IPAQ results confirmed that all participants reached, at a minimum, a moderate level of physical activity each week. Treadmill belt speeds were calculated from measurements of each participant's mean over ground comfortable walking speed during 2 min along an 11 m path with 180-degree turns at each end. Participants then walked on the treadmill with both belts at their typical walking speed (15 min) to familiarize to the treadmill and surroundings (*Tied-Belt Treadmill Familiarization*). Participants walked as they would on a day-to-day basis, with arms swinging naturally and gaze directed forwards. So that participants were aware of what speed changes may feel like and avoid any anxiety, two "splits", where one treadmill belt was slowed down (to 50% of their typical walking speed), were administered with ample warning (15 s).

2.4. FDG PET imaging sessions

Participants completed two, 2.5-h imaging visits to the laboratory and Brain Imaging Centre (Montreal Neurological Institute) (>48 h apart, mean 10 ± 10days). On each testing day, all participants fasted overnight (>6 h) to optimize cerebral ^{18}FDG uptake (Varrone et al., 2009). Participants repeated the *Tied-Belt Treadmill Familiarization* prior to ^{18}FDG injection on each imaging session to ensure walking comfort and a steady-state gait pattern was achieved.

A mean 188MBq bolus (±11MBq) of [^{18}F]-FDG was then injected into the cubital vein. Within 2 minutes (mean = 1.8 ± 0.5 minutes) of injection, participants began the treadmill walking trial. Upon uptake in the brain (heavily weighted towards the first 10–15 minutes after injection (Huang et al., 1980; Ginsberg et al., 1988)), ^{18}FDG is retained within cells, where it can be imaged using Positron Emission Tomography (PET). On each imaging session, participants performed one of two treadmill conditions for 30 min, ensuring optimal tracer uptake, with the order of treadmill conditions being randomized between participants (tied-belt and continuous adjustments, see below). Tracer accumulation while walking represents mean whole brain glucose metabolism, during each trial. Both conditions were performed on the same treadmill with the same visual and auditory surroundings.

The *tied-belt* walking condition was used as the reference task to account for any metabolic activity associated with typical walking and dynamic postural control during walking. During *tied-belt* walking, participants walked with both treadmill belts driven at their typical walking speed for 30 min.

The continuous adjustment condition was used as the experimental

task to isolate specific brain areas associated with ongoing changes to the gait pattern. During continuous adjustment, participants walked on the treadmill with the ratio of treadmill belt speeds changing every 15 s without warning to the participant for 30 min. Belt speeds at ratios of 100%, 50% or 33% of typical walking speed were randomly presented (See Fig. 1) and were frequent enough that participants continuously adjusted their gait to the treadmill. The order of belt speed changes was the same for all participants and ensured that the number of speed reductions were evenly applied to both sides. To confirm the perception of these belt changes, participants completed a short survey about belt speeds and belt speed changes after the PET imaging was completed. Due to software error during collection, gait data was not collected for 2 participants during the continuous adjustment condition.

2.5. PET and MRI acquisition

PET image acquisition began within 50 minutes of injection (mean 48 ± 7 minutes). This delay included the treadmill walking session (30 minutes), and a transition period for the participants to walk to the PET Imaging Centre at the Montreal Neurological Institute (MNI) (mean 5 ± 1 minutes). Actual PET scan acquisition duration was 40 min followed by an additional 10 min of transmission scan time for attenuation correction. The combined walking time, transition and imaging time was within the 110-min half-life of ^{18}F-FDG tracer (98 ± 7 min).

Images were obtained with a High-Resolution Research Tomograph (HRRT) PET scanner (CTI/Siemens, Knoxville, Tennessee) with a spatial resolution of 2.3–3.4 mm at full width half maximum (Funck et al., 2014). 3D sinograms were produced from the list-mode data acquired over 40 min and reformatted in a series of 8 successive 3D images of 5 min each. The use of 8 consecutive static images allowed for motion artefact correction. The 8 frames were then summed into a single 40-min long frame.

T1-weighted anatomical images of the brain were acquired for co-registration with PET images on a 3T Prisma Scanner (Siemens, Erlangen, Germany). A 3D magnetization rapid gradient echo was used (echo time: 2.98 ms; repetition time: 23 ms, flip angle = 9°) resulting in a voxel size of 1 × 1 × 1mm obtained across the entire brain using an echoplanar imaging sequence (field of view = 240 × 256mm^2).

2.6. PET image preprocessing

All PET images were processed and compared using Statistical Parametric Mapping 12 (SPM12, Welcome Trust Centre for Neuroimaging, Institute of Neurology, University College London, London, UK) running within MATLAB 2014b (MathWorks, Natick, Massachusetts, USA). Each condition's images (continuous adjustment or tied-belt) were linearly co-registered to the participant's native T1-weighted MR anatomical image. That MR study was co-registered and spatially normalized to the Montreal Neurological Institute template ICBM 152 6th generation linear brain atlas (Mazziotta et al., 2001). The 12-parameter affine transformation (Friston et al., 1995) allowing for co-registration of the subject's MR study to the template was then applied to the PET images already co-registered to the subject's MR in its native space, bringing both PET images into the MNI template space in a spatially normalized format. Using a Gaussian filter (Full width half Maximum = 8 mm), spatially normalized PET images were blurred to minimize noise. Radioactivity concentrations in [Bq/ml] were then normalized to the average radioactivity concentration in the white matter using a mask of the centrum semiovale in MNI space, generating white matter-normalized Standardized Uptake Value Ratios (SUVRs). This step was used to remove the effects of inter-subject non-test condition linked differences in radioactivity concentration prior to voxel-based statistics (la Fougere et al., 2010).

2.7. PET image statistical analysis

Whole Brain: Regional SUVRs were assessed for changes in brain activity during continuous walking adjustment compared to the tied-belt condition. To determine which brain regions are involved in the continuous alteration of the gait pattern, a flexible factorial design in SPM12 was used with treadmill condition (tied-belt, continuous adjustment) as the independent variable. Whole-brain group contrasts identified voxels of significant peak increase or decrease in glucose metabolism ($p < 0.005$, uncorrected (Tard et al., 2015)) and clusters of significant increase or decrease in glucose metabolism ($p < 0.05$, FDR correction, minimum 30 contiguous voxels). Participants' peak z-scores from each cluster were extracted for regression analysis. All stereotactic coordinates refer to the MNI coordinate system.

Region of Interest: Following whole brain analyses, a secondary hypothesis emerged for the deactivation of the DMN. To test whether clusters of deactivation were identified within the known DMN, a single mask of 10 mm spheres located at the DMN coordinates outlined by Andrews-Hanna et al. (2010) was created and a whole-brain group contrast was repeated specifically within this mask (Supplementary Fig. 2).

2.8. Gait analysis

The spatiotemporal gait outcomes analyzed were obtained directly from the Mobility Lab™ algorithms of the iWalk plugin for each gait cycle: 1) Cadence (steps per minute); 2) Stride Length (meters from heel

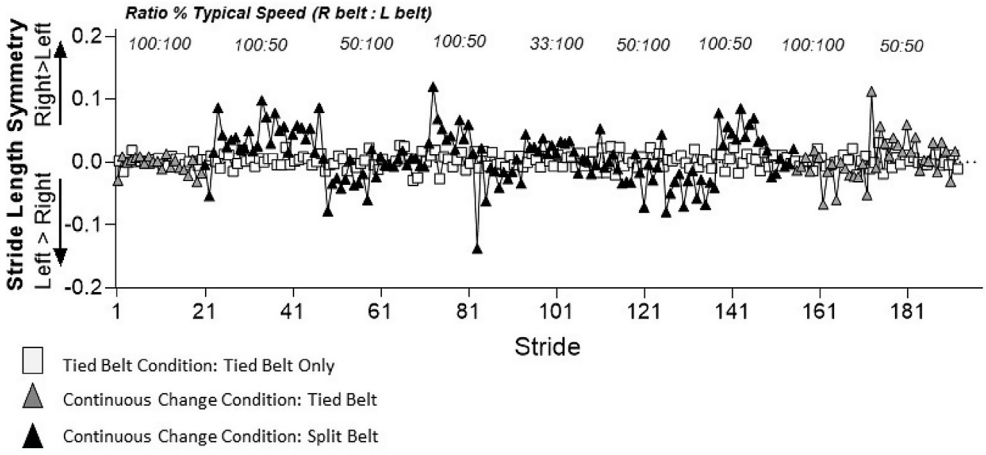

Fig. 1. Example of Step-to-Step Symmetry for one participant. While both belts remained at the participant's typical walking speed during tied-belt, the belt speed ratio was changed every 15 s during the continuous adjustment condition. The right and left belt speeds during the continuous adjustment condition are displayed as a percentage of typical speed, where 100% is equal to typical walking speed.

contact to heel contact of the same leg) and 3) Proportion of the gait cycle spent in dual support. A relative measure of dual support was calculated based on which leg was approaching terminal stance: for instance left leg dual support occurred from right-foot heel contact to left-foot toe-off (Reisman et al., 2005). Dual support for each leg was then expressed as a proportion of the gait cycle time (% GCT).

Gait symmetry was assessed as the difference in performance in terms of stride length and dual support between each leg, presented as a ratio of the combined performance of both legs for that gait cycle (Step Symmetry = (Right Leg–Left Leg)/(Right Leg + Left Leg)). A symmetry value of 0 indicates both legs performed at exactly the same level (Malone and Bastian, 2010). To account for any inherent bias in each participant's gait symmetry, a mean symmetry was calculated from the first minute of tied-belt walking of each testing day and removed from all data points in the gait trial post-injection.

Learning (i.e. adaptation to split-belts) did not occur during the continuous adjustment trial (stride length symmetry- 1st minute: 0.05 ± 0.03; 15th minute: 0.05 ± 0.02; 29th minute: 0.04 ± 0.02 $p > 0.05$; dual support symmetry- 1st minute: 0.11 ± 0.04; 15th minute: 0.10 ± 0.02; 29th minute: 0.11 ± 0.04 $p > 0.05$) so each participant's mean and standard deviation (SD) of stride length symmetry and dual support symmetry were calculated across the entire 30-min trial to compare treadmill conditions. To further describe global stride-to-stride variability of symmetry measures, the proportion of steps (%total) each participant took beyond 2 SD of the tied-belt mean was calculated for both the tied-belt walking and continuous adjustment trial. Finally, to assess whether [^{18}F]-FDG uptake was altered by the frequency of stepping, the percentage change in cadence from the tied-belt to continuous adjustment trial was calculated for each participant.

2.9. Gait statistical analysis

To determine overall differences in gait symmetry between treadmill conditions, one-way repeated measures ANOVAs were used to detect an effect of treadmill type (tied-belt, continuous adjustment) for 1) mean; 2) SD; and 3) number of steps outside 2SD threshold of each outcome measurement (dual support and stride length symmetry) for a total of 6 separate one-way ANOVA. Statistical tests were completed in SPSS Version 22 and deemed significant at $p < 0.05$.

To determine if a relationship existed between individual participant's FDG uptake and their gait pattern, bivariate Pearson's correlations were calculated between participants' peak Z score within clusters of increased and decreased FDG uptake (determined from group level analyses) and gait outcome variables (%change in cadence from tied-belt walking, %steps outside tied-belt walking threshold, SD of symmetry measures). A linear regression was calculated to model participants' peak Z score within each significant cluster based on gait outcomes with significant correlations, corrections for multiple regressions were not applied. The regressions were assessed in SPSS Version 22 and deemed significant at $p < 0.05$.

2.10. Data availability

The data that support the findings of this study are available upon request.

3. Results

3.1. Gait modifications required for continuous adjustment condition

The continuous adjustment condition successfully increased stride-to-stride variability beyond typical walking and required participants to alter their gait pattern in response to belt speed changes (Fig. 1). Mean stride length symmetry and dual support symmetry were similar between conditions (Fig. 2A, $p > 0.05$), however stride-to-stride symmetry variability increased during the continuous adjustment condition compared to the tied-belt (Fig. 2 B–C, $p < 0.05$). Standard deviation of participants' mean gait symmetry across all gait cycles were significantly greater during the continuous adjustment trial (Fig. 2B: stride length: $F(1,7) = 254.989, p < 0.001$, dual support: $F(1,7) = 504.652, p < 0.001$). Participants spent a significantly greater percentage of strides outside of 2 standard deviations of their typical tied-belt gait symmetry pattern during the continuous adjustment trial than during tied-belt walking (Fig. 2C: stride length: $F(1,7) = 20.975, p < 0.001$; dual support:$F(1,7) = 43.060, p < 0.001$).

While all participants felt they walked as they typically do during the tied-belt condition (1.14 ± 0.05 m/s), 8 of 10 participants felt they were not able to use their typical walking pattern during the continuous adjustment condition. All participants perceived belt speed ratio changes during the continuous adjustment trial, with 9 of 10 participants reporting that they thought these changes occurred every 30 s or less. Six of 10 participants reported they believed they could predict when the next belt speed change would occur, but not which leg would change.

3.2. Changes of brain metabolism regional distribution during continuous gait adjustments on the split-belt treadmill

During continuous gait pattern adjustments, in contrast with tied-belt treadmill walking, significant clusters of increased metabolism ($p < 0.05$ FDR corrected, Fig. 3, Supplementary Table 1) were found in the right PPC (Brodmann Area (BA) 5,7), right anterior cingulate gyrus (ACC, BA24), bilateral SMA (BA6) and left lateral cerebellum (lobules VI,VIII). Significant peaks of increased glucose uptake were also noted in the right insula, right inferior parietal lobe, the right precentral gyrus, the right thalamus and bilateral cerebellum ($p < 0.005$, uncorrected).

A significant decrease in peak metabolism during continuous adjustments (compared to tied-belt walking) was found in the left posterior cingulate cortex (BA23, 31) ($p < 0.005$ uncorrected, Fig. 4, Supplementary Table 2). There was also evidence of a significant decrease in peak glucose metabolism in the left medial pre-frontal cortex (PFC), right ACC, left precuneus, right frontal gyrus and left superior temporal gyrus. To further explore and confirm these deactivations, specific region of interest analyses within areas known to be part of the DMN were performed. These secondary analyses further supported that the peak of activity decrease of the left posterior cingulate and inferior parietal cortex were both within the DMN, a known functional connectivity network (See Supplementary Table 3, Supplementary Fig. 2 (Andrews-Hanna et al., 2010)).

3.3. Associations between gait performance and neural correlates of continuous adjustments

A significant decrease in cadence from tied-belt cadence (a value of 0) was associated with a further increase of the PPC cluster. Compared to tied-belt walking, participants' increase in peak Z score within the cluster of right PPC activation during continuous adjustment was associated with a decrease in change in cadence (Z score = −6.445×%change cadence+2.362; $F(1,6) = 16.15$, $p = 0.007$, $R^2 = 0.7291$, Fig. 5A).

A greater SMA cluster activation was associated with greater dual support symmetry variability. Compared to tied-belt walking, participant's increase in peak Z score within the cluster of the left SMA was associated with an increase in dual support symmetry SD (Z score = 89.4 × dual support symmetry standard devation–1.791, $p = 0.0419$, $R^2 = 0.5256$, Fig. 5B).

Finally, participants who had the greatest peak deactivation of the PFC cluster showed the lowest proportion of steps with a stride length symmetry outside of the tied-belt treadmill walking threshold. Compared to tied-belt walking, increases in the percentage of steps outside of 2 standard deviation of the tied-belt mean were associated with decreased peak Z score within the left medial PFC (Z score = −0.03579 × % change+5.295; $F(1,6) = 7.154$, $p = 0.0368$, $R^2 = 0.5439$; Fig. 5C).

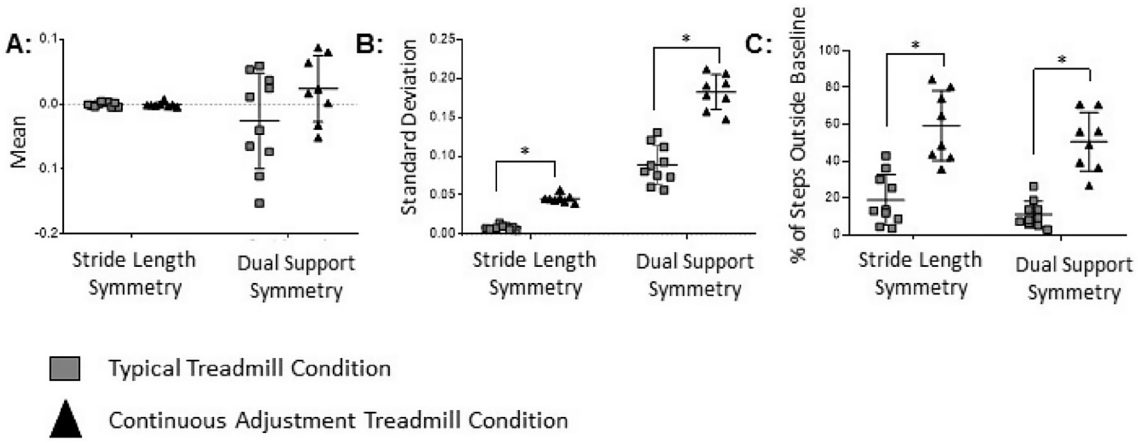

Fig. 2. Walking performance. Individual data points represent each participant. The group mean ± 1SE is represented with a solid line. **A)** Mean gait symmetry was not different between conditions ($p > 0.05$). **B)** Gait symmetry standard deviation was greater during continuous adjustment ($p < 0.05$). **C)** Participants had a significantly greater proportion of steps beyond 2 standard deviations of tied-belt mean during the continuous adjustment trial ($p < 0.05$).

4. Discussion

Our results indicate that when modifications to the gait pattern are required in response to unpredictable environmental perturbations, a distributed network across the entire brain is recruited (See Fig. 6): there is increased activity of SMA, PPC, anterior cingulate cortex and anterior lateral cerebellum, and decreased activity of posterior cingulate and medial prefrontal cortex. In addition, peak activation of the PPC, SMA and PFC were correlated with cadence and temporal gait variability. Expanding on the network proposed by la Fougere and colleagues (la Fougere et al., 2010) we propose that error-driven sensorimotor feedback from lateral cerebellar lobule VI is relayed to cortical regions responsible for sensorimotor integration (PPC), motor planning (SMA) and goal directed attention (ACC) to inform any required changes to the motor program from the primary motor cortex. Activity from medial prefrontal cortex (mPFC) and posterior cingulate cortex (PCC) decreases relative to typical walking, likely as an active release to direct cortical resource flow to motor planning regions. This proposed "fine-tuning" pathway for locomotion depicts changes in activity relative to typical, steady-state, treadmill walking.

4.1. Lateral cerebellum relays error-driven movement feedback to update locomotor plan

Our results provide direct evidence of what a variety of split belt adaptation protocols have previously hypothesized: the important role of the cerebellum in adjusting gait to asymmetrical belt speeds (Bastian, 2006; Morton and Bastian, 2006; Malone and Bastian, 2010). As expected, participants increased recruitment of lateral cerebellar areas, specifically Lobules VI and VIII outside of the cerebellar vermis, during unpredictable step-to-step gait pattern changes. The cerebellum is a major hub of confluent information from both the spinal cord for sensory feedback and cortical regions for feedforward control (Takakusaki, 2013). Lobule VI receives input from and projects output to the primary motor cortex via the pontine and dentate nuclei and thalamus and thus has been hypothesized to be primarily a sensorimotor region of the cerebellum (Glickstein et al., 1985; Kelly and Strick, 2003) and a movement error sensor (Kitazawa et al., 1998; Imamizu et al., 2000; Diedrichsen et al., 2005).

Increased activity in the cerebellum during gait modification aligns with the hypothesis of the cerebellum as an error driven and feedforward sensor (Bastian, 2006). In the context of walking, this area is thought to be involved in motor learning and updating of the internal locomotor plan (Imamizu et al., 2000). During locomotion, cerebellar climbing fibres increase their activity, coding for predicted error severity during the stance portion of the perturbed leg and the swing phase of the next step, and allowing for planning of the next foot placement (Yanagihara and Udo, 1994). Finally, damage within the cerebellar hemispheres makes gait adaptation to split-belts (i.e. learning) impossible (Morton and

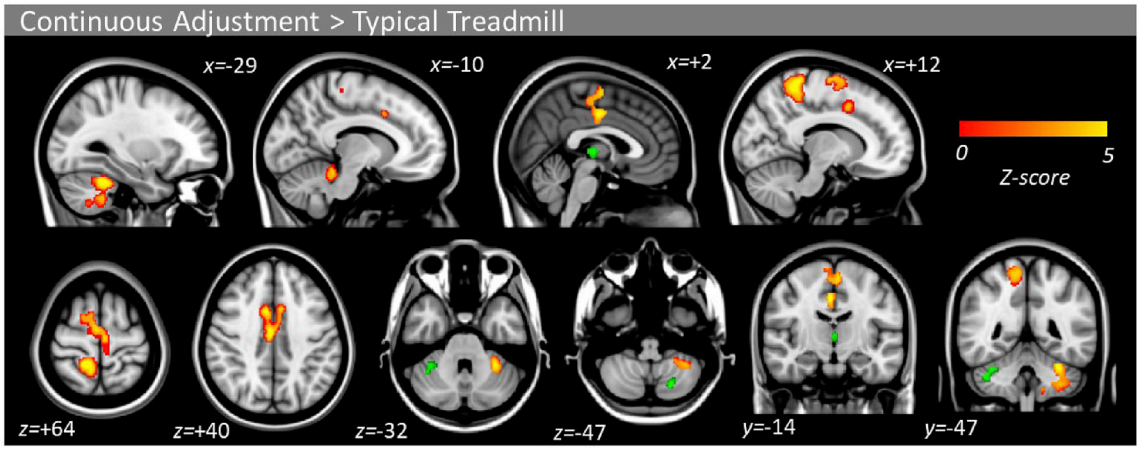

Fig. 3. Activation maps for continuous adjustment of gait. Compared to tied-belt walking, the continuous adjustment trial significantly increased glucose uptake in a cluster (FDR corrected $p<0.05$) in the left posterior parietal cortex, left anterior cingulate cortex, bilateral supplementary motor areas and right anterior cerebellum (Lobule VI, VIII). Significant increases in peak glucose uptake ($p<0.005$ uncorrected) are shown with green.

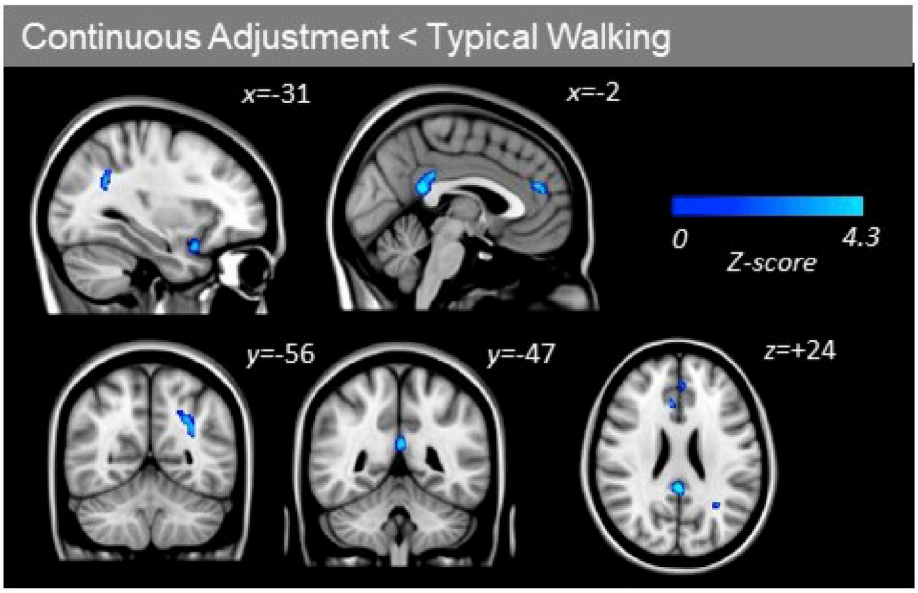

Fig. 4. Deactivation maps for continuous adjustment of gait. Compared tied-belt treadmill walking, the continuous gait adjustment trial significantly decreased peak glucose uptake ($p < 0.005$ uncorrected) in a in the left posterior cingulate gyrus and left medial prefrontal cortex. Z-scores depicted are $p < 0.005$ uncorrected.

Bastian, 2006). Though our participants were never at a belt ratio long enough to show gait pattern adaptation, we believe that this lateral cerebellar activation is a result of an accumulation of 30 min of attempting to integrate ongoing changes to the locomotor plan.

4.2. Posterior parietal cortex activation for reactive gait adjustments

While previous work has demonstrated a change in PPC activity during obstacle avoidance in cat locomotion, additional PPC activation has not previously been hypothesized during unpredictable human gait modification or adjustments to split-belt treadmill walking. We suggest this activation would complement feedback from lateral cerebellum to inform updates to the locomotor plan. It is likely that the PPC activation during these gait adjustments reflects an increased associative workload needed to integrate visual and proprioceptive information with the ensuing movement of each leg. During direct electrophysiological recordings in the PPC of walking cats, BA 5 increased activity during obstacle avoidance with obstacles held in working memory (Lajoie et al., 2010; Drew and Marigold, 2015), obstacle avoidance with and without tactile feedback (Wong and Lomber, 2018), and obstacle avoidance without visual information (Marigold and Drew, 2011). Given that proprioceptive information from the feet would be especially important during treadmill walking, being one of the first sensory cues of a belt speed change, our results support the hypothesis that the PPC actively participates in integrating sensory information for specifying motor outputs for the upcoming step in the human CNS.

In humans, the PPC has also been suggested to generate a body schema that would be responsible for integrating limb movement, and their movements relative to the body, with information about the environment (Takakusaki, 2013). During continuous belt speed changes, a body schema representation would likely incorporate sensorimotor feedback from each leg separately based on both placement and timing into modifications of the motor plan for upcoming steps. In addition, activations of the PPC together with the ACC and SMA, are thought to be involved in visuo-motor integration and error monitoring (Gwin et al., 2011). The use of the PPC for sensory integration, body schema error monitoring and holding environmental constraints in working memory would allow the PPC to assist the SMA and primary motor cortices in selecting subsequent locomotor plan updates (Drew and Marigold, 2015). Indeed, by integrating real-time signals of sensory feedback to the body schema, information can then be passed on the SMA for motor program updates and planning for upcoming steps (Lajoie et al., 2010).

4.3. The supplementary motor area and anterior cingulate cortex participate in updating the locomotor plan

In conjunction with PPC activity, our results suggest that SMA and ACC activations are required for fine-tuning the stepping pattern in response to a change to the belt speed ratio. In fact, participants with the greatest between-step changes to gait phasing also had the greatest overall increase in SMA activity, supporting the role of SMA for fine-tuning gait modifications. Brain activation studies during gait have pointed to the SMA's role in motor planning, motor programming for voluntary movements and maintaining rhythmic stepping (Fukuyama et al., 1997; Harada et al., 2009). SMA activity increased just prior to both routine and precision stepping, without further change during the actual execution of these tasks (Koenraadt et al., 2014) pointing to a role for the SMA in movement initiation planning which became significantly more complex in our continuous gait change protocol.

It is well understood that the ACC increases its activity for focused attention and cognitive processing selection (Pardo et al., 1990). In addition, the ACC was shown to be linked to foot placement monitoring and ongoing error correction (Bush et al., 2000; Gwin et al., 2011) as well as to be active just prior to a goal directed movement (Cole and Schneider, 2007). In conjunction with PPC and SMA, ACC activity would allow the nervous system to implement updates to stance and swing as appropriate to the environment (i.e. the belt speed under each foot in our protocol). As participants do not know the exact moment of the belt speed changes, one possible explanation to the increase in SMA and ACC activity would be that those structures are primarily required for online adjustment and anticipation of a possible fine tuning of the gait pattern in response to a belt speed change.

4.4. Continuous gait adjustments further reduced activation of the default mode network

Our findings re-emphasize the ability of the healthy CNS to reduce DMN activity during motor task performance. Involved in self-reference, memory and thought, the DMN is active at rest (Raichle et al., 2001) and

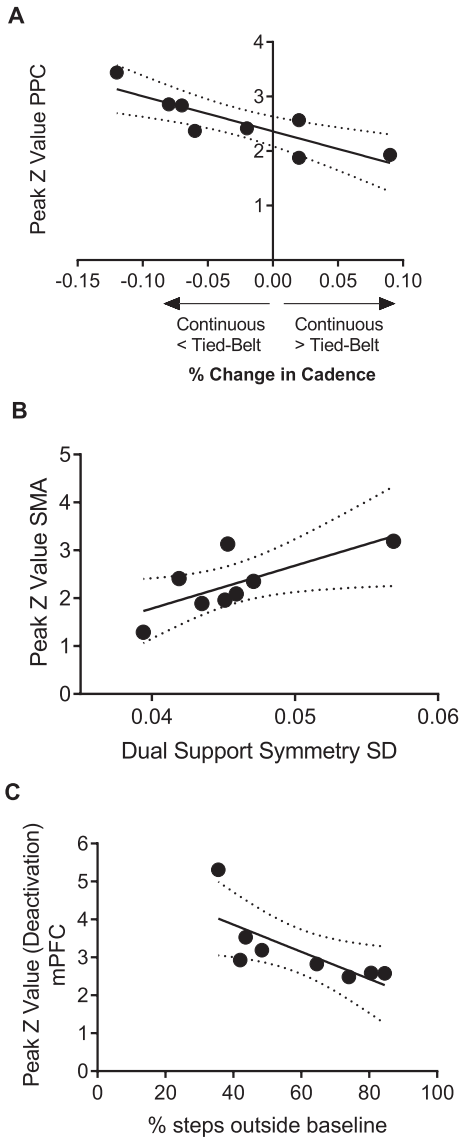

Fig. 5. Correlation between activated regions and gait parameters. A: A decrease in participants' cadence from the tied-belt to continuous adjustment trial was significantly related to an increase in peak activity (Z score) of the PPC cluster ($p < 0.05$). Participants who increased cadence from the tied-belt to continuous adjustment trial, had a significant decrease in peak activity (Z score) of the PPC cluster ($p < 0.05$). **B:** An increase in participants' dual support symmetry variability (continuous adjustment trial) was significantly related to an increase in peak activity (Z score) in the SMA cluster ($p < 0.05$). **C:** A decrease in participants' percentage of steps outside of the tied-belt threshold (mean ± 2SD), that is lower variability, was related to a decrease in peak activity (Z score) in the PFC cluster ($p < 0.05$). Dotted lines indicate a 95% confidence interval.

deactivates to some extent with any movement, including walking (Crockett et al., 2017). More specifically, deactivation of the posterior cingulate was also related to feelings of undistracted attention or letting go of directed task-related attention (Garrison et al., 2013) and could act as a potential cognitive release to allow motor and motor planning areas to alter the ongoing locomotor plan. The medial PFC is typically discussed as a regulator of higher cognitive input and/or executive functions (Koechlin and Hyafil, 2007) and typically increases its activity with new experience. However with exploration of a repeated task and using feedback to reduce error, this area has been shown to decrease its activity (Koechlin et al., 2002). In fact, participants who reduced activity the most within the medial PFC cluster during continuous adjustments were

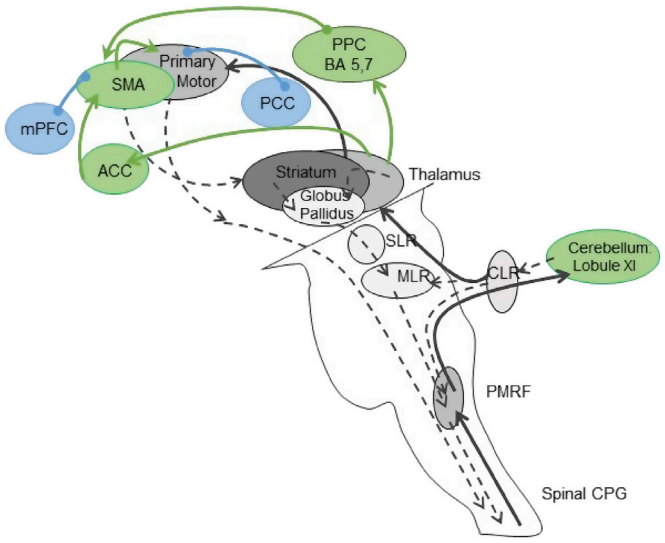

Fig. 6. The "fine-tuning" network of locomotion. Step-to-step gait pattern changes require increased activity (green) and decreased activity (blue) of cortical regions compared to typical walking (grey). This model elaborates on the "executive" and "planning" networks of locomotion proposed by la Fougere et al. (2010). SLR: subthalamic locomotor region; MLR: mesencephalic locomotor region; CLR: cerebellar locomotor region; PMRF: pontine and medullary reticular formations; CPG: Central Pattern Generator.

least variable in their stride-to-stride placement. Given the participants' high step-to-step variability imposed by the split-belt task, they were less able to predict belt speed changes and instead had to use on-the-fly sensory information as it was processed to implement gait pattern changes. In doing so, the less the participants used higher order cognitive resources to attend to the ongoing treadmill changes, the more control their neural system was able to exert on a stride-by-stride basis. Within this hypothesis, activation of the PFC would likely only impede or slow down this sensory integration and ensuing step-to-step changes therefore is unnecessary or even counterproductive.

4.5. Study limitations

While FDG-PET imaging provides excellent spatial resolution, its temporal resolution is limited to the entire uptake period and we cannot comment on specific gait cycle events or time points within the uptake period. As we chose to look at the neural activity associated with step-to-step gait adjustments, we selected tied-belt walking as our reference task and we cannot comment on brain activity required for typical treadmill walking on its own.

5. Conclusion

We propose that a "fine-tuning" network for human locomotion exists which includes brain areas for sensorimotor integration, motor planning and goal directed attention. While some areas increase in activity relative to typical treadmill walking (cerebellum lobule VI, PPC, SMA, ACC), others act as a cognitive release and decrease in activity relative to typical treadmill walking (posterior cingulate gyrus, medial PFC). Ongoing and flexible changes to the walking pattern are made through error detection and visuo-motor and tactile sensory integration. Gait pattern changes are facilitated by a deactivation higher order cognitive control, liberating resources for motor planning and execution. These findings point to the inherent flexibility of the human locomotor plan to react and adjust to environmental changes, updating its activity as information arrives from current motor activity in order to optimize performance during the upcoming step, maintaining a successful walking pattern.

Funding

This study was supported by a Natural Sciences and Engineering Research Council of Canada (NSERC) Discovery Grant (CP), a Canadian Foundation for Innovation Grant (CP), an NSERC Post Graduate Scholarship (DH), a Fonds de Recherche en Santé de Québec Doctoral Scholarship (DH), and a Healthy Brains for Healthy Lives McGill University Doctoral Fellowship (DH).

Conflicts of interest

The authors declare no competing financial interests.

Acknowledgements

We gratefully acknowledge the research technicians from the McConnell Brain Imaging Centre at the Montreal Neurological Institute (PET and MR Imaging Centres) for their help with data collection.

Appendix A. Supplementary data

Supplementary data to this article can be found online at https://doi.org/10.1016/j.neuroimage.2019.116095.

References

Bastian, A.J., 2006. Learning to predict the future: the cerebellum adapts feedforward movement control. Curr. Opin. Neurobiol. 16 (6), 645–649. https://doi.org/10.1016/j.conb.2006.08.016.

Bastian, A.J., Mink, J.W., Kaufman, B.A., Thach, W.T., 1998. Posterior vermal split syndrome. Ann. Neurol. 44, 601–610.

Andrews-Hanna, J.R., Reidler, J.S., Sepulcre, J., Poulin, R., Buckner, R.L., et al., 2010. Functional-anatomic fractionation of the brain's default network. Neuron 65 (4), 550–562. https://doi.org/10.1016/j.neuron.2010.02.005.

Billingston, J., Wilkie, R.M., Wann, J.P., 2013. Obstacle avoidance and smooth trajectory control: neural areas highlighted during improved locomotor performance. Front. Behav. Neurosci. 7 (9) https://doi.org/10.3389/fnbeh.2013.00009.

Blanchette, A., Bouyer, L.J., 2009. Timing-specific transfer of adapted muscle activity after walking in an elastic force field. J. Neurophysiol. 102 (1), 568–577. https://doi.org/10.1152/jn.91096.2008.

Bush, G., Luu, P., Posner, M.I., 2000. Cognitive and emotional influences in anterior cingulate cortex. Trends Cogn. Sci. 215–222.

Choi, J.T., Vining, E.P.G., Reisman, D.S., Bastian, A.J., 2009. Walking flexibility after hemispherectomy: split-belt treadmill adaptation and feedback control. Brain 132, 722–733.

Cole, M.W., Schneider, W.J.N., 2007. The cognitive control network: integrated cortical regions with dissociable functions. Neuroimage 37, 343–360.

Craig, C.L., Marshall, A., Sjostrom, M., Bauman, A.E., Booth, M.L., Ainsworth, B.E., Pratt, M., et al., 2003. Med. Sci. Sport. Eexercise 35 (8), 1381–1395.

Crockett, R.A., Hsu, C.L., Best, J.R., Liu-Ambrose, T., 2017. Resting State default Mode network connectivity, dual task performance, gait speed, and postural sway in older adults with mild cognitive impairment. Front. Aging Neurosci. 9, 423.

Diedrichsen, J., Hashambhoy, Y., Rane, T., Shadmehr, R., 2005. Neural correlates of reach errors. J. Neurosci. 25, 9919–9931.

Dietz, V., Zijlstra, W., Prokop, T., 1995. Leg muscle activation during gait in Parkinson's disease: adaptation and interlimb coordination. Electroencephalograp. Clin. Neurophysiol./Electromyograp. Motor Contr. 97 (6), 408–415.

Drew, T., Marigold, D.S., 2015. Taking the next step: cortical contributions to the control of locomotion. Curr. Opin. Neurobiol. 33, 25–33.

Friston, K.J., Ashburner, J., Frith, C.D., Poline, J.B., Heather, J.D., Frackowiak, R.S.J., 1995. Spatial registration and normalization of images, 3, 165–189.

Fukuyama, H., Ouchi, Y., Matsuzaki, S., Nagahama, Y., Yamauchi, H., Ogawa, M., Kimura, J., Shibasaki, H., 1997. Brain functional activity during gait in normal subjects: a SPECT study. Neurosci. Lett. 228, 183–186.

Funck, T., Paquette, C., Evans, A., Thiel, A., 2014. Surface-based partial-volume correction for high-resolution PET. Neuroimage 102 Pt 2, 674–687.

Garrison, K., Juan Santoyo, Jake Davis, Thornhill, T., Catherine, K., Judson, B., 2013. Effortless awareness: using real time neurofeedback to investigate correlates of posterior cingulate cortex activity in meditators' self-report. Front. Human Neurosci. 7, 440.

Ginsberg, M.D., Chang, J.Y., Kelley, R.E., Yoshii, F., Barker, W.W., Ingenito, G., Boothe, T.E., 1988. Increases in both cerebral glucose utilization and blood flow during execution of a somatosensory task. Ann. Neurol.: Off. J. Am. Neurol. Assoc. Child Neurol. Soc. 23, 152–160.

Glickstein, M., May III, J.G., Mercier, B.E., 1985. Corticopontine projection in the macaque: the distribution of labelled cortical cells after large injections of horseradish peroxidase in the pontine nuclei. J. Comp. Neurol. 235, 343–359.

Gwin, J.T., Gramann, K., Makeig, S., Ferris, D.P., 2011. Electrocortical activity is coupled to gait cycle phase during treadmill walking. Neuroimage 54, 1289–1296.

Harada, T., Miyai, I., Suzuki, M., Kubota, K., 2009. Gait capacity affects cortical activation patterns related to speed control in the elderly. Exp. Brain Res. 193, 445–454.

Huang, S.-C., Phelps, M.E., Hoffman, E.J., Sideris, K., Selin, C.J., Kuhl, D.E., 1980. Noninvasive determination of local cerebral metabolic rate of glucose in man. Am. J. Physiol. Endocrinol. Metabol. 238, E69–E82.

Ilg, W., Giese, M., Gizewski, E., Schoch, B., Timmann, D.J.B., 2008. The influence of focal cerebellar lesions on the control and adaptation of gait, 131, 2913–2927.

Imamizu, H., Miyauchi, S., Tamada, T., Sasaki, Y., Takino, R., Putz, B., Yoshioka, T., Kawato, M., 2000. Human cerebellar activity reflecting an acquired internal model of a new tool. Nature 403, 192–195.

Kelly, R.M., Strick, P.L., 2003. Cerebellar loops with motor cortex and prefrontal cortex of a nonhuman primate. J. Neurosci. 23, 8432–8444.

Kitazawa, S., Kimura, T., Yin, P.B., 1998. Cerebellar complex spikes encode both destinations and errors in arm movements. Nature 392, 494–497.

Koechlin, E., Hyafil, A.J.S., 2007. Anterior prefrontal function and the limits of human decision-making, 318, 594–598.

Koechlin, E., Danek, A., Burnod, Y., Grafman, J.J.N., 2002. Medial prefrontal and subcortical mechanisms underlying the acquisition of motor and cognitive action sequences in humans, 35, 371–381.

Koenraadt, K.L., Roelofsen, E.G., Duysens, J., Keijsers, N.L., 2014. Cortical control of normal gait and precision stepping: an fNIRS study. Neuroimage 85, 415–422. Pt 1.

la Fougere, C., Zwergal, A., Rominger, A., Forster, S., Fesl, G., Dieterich, M., Brandt, T., Strupp, M., Bartenstein, P., Jahn, K., 2010. Real versus imagined locomotion: a [18F]-FDG PET-fMRI comparison. Neuroimage 50, 1589–1598.

Lajoie, K., Andujar, J.E., Pearson, K., Drew, T., 2010. Neurons in area 5 of the posterior parietal cortex in the cat contribute to interlimb coordination during visually guided locomotion: a role in working memory. J. Neurophysiol. 103, 2234–2254.

Malone, L.A., Bastian, A.J., 2010. Thinking about walking: effects of conscious correction versus distraction on locomotor adaptation. J. Neurophysiol. 103, 1954–1962.

Marigold, D.S., Drew, T., 2011. Contribution of cells in the posterior parietal cortex to the planning of visually guided locomotion in the cat: effects of temporary visual interruption. J. Neurophysiol. 105, 2457–2470.

Mazziotta, J., et al., 2001. A probabilistic atlas and reference system for the human brain: International Consortium for Brain Mapping (ICBM). Philos. Trans. R. Soc. Lond. Ser. B Biol. Sci. 356, 1293–1322.

Mitchell, T., Faryn Starrs, Jean-Paul Soucy, Thiel, A., 2018. and Caroline Paquette. "Impaired sensorimotor processing during complex gait precedes behavioral changes in middle-aged adults. J. Gerontol.: Ser. A.

Mitchell, T., Potvin-Desrochers, A., Lafontaine, A.-L., Monchi, O., Thiel, A., Paquette, C., 2018b. Cerebral metabolic changes related to freezing of gait in Parkinson's disease. J. Nuclear Med. 60 (5), 671–676. https://doi.org/10.2967/jnumed.118.218248.

Miyai, I., Tanabe, H.C., Sase, I., Eda, H., Oda, I., Konishi, I., Tsunazawa, Y., Suzuki, T., Yanagida, T., Kubota, K., 2001. Cortical mapping of gait in humans: a near-infrared spectroscopic topography study. Neuroimage 14, 1186–1192.

Morton, S.M., Bastian, A.J., 2006. Cerebellar contributions to locomotor adaptations during splitbelt treadmill walking. J. Neurosci. : Off. J. Soc. Neurosci. 26, 9107–9116.

Pardo, J.V., Pardo, P.J., Janer, K.W., Raichle, M.E., 1990. The anterior cingulate cortex mediates processing selection in the Stroop attentional conflict paradigm. Proc. Natl. Acad. Sci. 87, 256–259.

Raichle, M.E., MacLeod, A.M., Snyder, A.Z., Powers, W.J., Gusnard, D.A., Shulman, G.L., 2001. A default mode of brain function. Proc. Natl. Acad. Sci. U. S. A. 98, 676–682.

Reisman, D.S., Block, H.J., Bastian, A.J., 2005. Interlimb coordination during locomotion: what can be adapted and stored? J. Neurophysiol. 94, 2403–2415.

Reisman, D.S., Bastian, A.J., Morton, SMJPt, 2010. Neurophysiologic and rehabilitation insights from the split-belt and other locomotor adaptation paradigms, 90, 187–195.

Suzuki, M., Miyai, I., Ono, T., Kubota, K., 2008. Activities in the frontal cortex and gait performance are modulated by preparation. An fNIRS study. Neuroimage 39, 600–607.

Takakusaki, K., 2013. Neurophysiology of gait: from the spinal cord to the frontal lobe. Mov. Disord. : Off. J. Mov. Disord. Soc. 28, 1483–1491.

Tard, C., Delval, A., Devos, D., Lopes, R., Lenfant, P., Dujardin, K., Hossein-Foucher, C., Semah, F., Duhamel, A., Defebvre, L.J.N., 2015. Brain Metabolic Abnormalities during Gait with Freezing in Parkinson's Disease, vol. 307, pp. 281–301.

Varrone, A., Asenbaum, S., Vander Borght, T., Booij, J., Nobili, F., Nagren, K., Darcourt, J., Kapucu, O.L., Tatsch, K., Bartenstein, P., Van Laere, K., 2009. EANM procedure guidelines for PET brain imaging using [18F]FDG, version 2. Eur. J. Nucl. Med. Mol. Imaging 36, 2103–2110.

Wong, C., Lomber, S.G.J.C.B., 2018. Stable Delay Period Representations in the Posterior Parietal Cortex Facilitate Working-Memory-Guided Obstacle Negotiation.

Wong, C., Lomber, S.G., 2019. Stable Delay Period Representations in the Posterior Parietal Cortex Facilitate Working-Memory-Guided Obstacle Negotiation. Curr. Biol. 29 (1), 70–80.

Yanagihara, D., Udo, M., 1994. Climbing fiber responses in cerebellar vermal Purkinje cells during perturbed locomotion in decerebrate cats. Neurosci. Res. 19 (2), 245–248.

Yang, J.F., Lamont, E.V., Pang, M.Y., 2005. Split-belt treadmill stepping in infants suggests autonomous pattern generators for the left and right leg in humans. J. Neurosci. 25 (29), 6869–6876.